



A targeted disruption of the murine *Brcal* gene causes γ -irradiation hypersensitivity and genetic instability

Shan-Xiang Shen¹, Zoë Weaver², Xiaoling Xu¹, Cuiling Li¹, Michael Weinstein¹, Lin Chen¹, Xin-Yuan Guan³, Thomas Ried² and Chu-Xia Deng¹

¹Laboratory of Biochemistry and Metabolism, National Institute of Diabetes, Digestive and Kidney Diseases, Building 10, 9N105; ²Genome Technology Branch; ³Laboratory of Cancer Genetics, National Human Genome Research Institute, National Institutes of Health, Bethesda, Maryland 20892, USA

Germline mutations of the *Brcal* gene are responsible for most cases of familial breast and ovarian cancers, but somatic mutations are rarely detected in sporadic events. Moreover, mouse embryos deficient for *Brcal* have been shown to die during early embryogenesis due to a proliferation defect. These findings seem incompatible with the tumor suppress function assigned to this gene and raise questions about the mechanism by which *Brcal* mutations cause tumorigenesis. We now directly demonstrate that BRCA1 is responsible for the integrity of the genome. Murine embryos carrying a *Brcal* null mutation are developmentally retarded and hypersensitive to γ -irradiation, suggesting a failure in DNA damage repair. This notion is supported by spectral karyotyping (SKY) of metaphase chromosomes, which display numerical and structural aberrations. However, massive chromosomal abnormalities are only observed when a p53^{-/-} background is introduced. Thus, a p53 dependent cell cycle checkpoint arrests the mutant embryos and prevents the accumulation of damaged DNA. *Brcal*^{-/-} fibroblasts are not viable, nor are *Brcal*^{-/-}:p53^{-/-} fibroblasts. However, proliferative foci arise from *Brcal*^{-/-}:p53^{-/-} cells, probably due to additional mutations that are a consequence of the accumulating DNA damage. We believe that the increased incidence of such additional mutations accounts for the mechanism of tumorigenesis associated with *Brcal* mutations in humans.

Keywords: BRCA1; p53; radiation sensitivity and chromosome abnormality

Introduction

Breast cancer is the most common cancer and the second leading cause of cancer mortality in women (Alberg and Helzlsouer, 1997; Hill *et al.*, 1997). About 3–5% of the breast cancer cases are believed to be heritable (Hill *et al.*, 1997). Two cancer susceptibility genes, *Brcal* (Miki *et al.*, 1994) and *Brcal2* (Wooster *et al.*, 1995) have been discovered. Mutations in the *Brcal* and *Brcal2* genes represent most cases of hereditary breast cancers (Casey, 1997), and mutations in *Brcal* were also found to be related to an increased risk for other cancers (Casey, 1997).

The human *Brcal* gene encodes a nuclear protein of 1863 amino acids which was recently shown to co-

localize and co-immunoprecipitate with RAD 51, a homolog of *E. Coli* RecA that is involved in DNA damage repair (Muris *et al.*, 1993; Scully *et al.*, 1997a,b; Shinohara *et al.*, 1993, 1992). Upon treatment with reagents that damage DNA, BRCA1 becomes phosphorylated and relocates to intranuclear structures in which DNA replication is taking place (Scully *et al.*, 1997a). While these findings suggest an involvement of BRCA1 in DNA damage repair, the function of BRCA1 in mediating genomic stability has not been illustrated.

The mouse *Brcal* gene encodes a protein of 1812 amino acids with about 58% identity to the human protein. The function of murine *Brcal* has been studied by targeted gene disruptions in embryonic stem (ES) cells followed by germline transmission. It was shown that mice that were heterozygous for the targeted mutations were normal whereas the homozygotes died between embryonic day 6–13.5 (E6–13.5) (Gowen *et al.*, 1996; Hakem *et al.*, 1996; Liu *et al.*, 1996). In most cases, the mutations of BRCA1 are associated with a severe developmental delay and a cellular proliferation defect (Hakem *et al.*, 1996; Liu *et al.*, 1996; Ludwig *et al.*, 1997). It was recently shown that the early lethality of BRCA1^{-/-} embryos could be partially rescued by a p53-null or p21-null mutation, suggesting that loss of BRCA1 may trigger the activation of a cell cycle checkpoint (Hakem *et al.*, 1997; Ludwig *et al.*, 1997). However, the mechanism that causes such an activation has not been demonstrated.

In the present study, we have directly demonstrated that murine BRCA1 is responsible for genomic integrity as *Brcal*^{-/-} embryos exhibited hypersensitivity to γ -irradiation and chromosomal abnormalities. We also found that the loss of p53 is not itself sufficient to allow for the growth of *Brcal*^{-/-} embryonic fibroblast cells. It does, however, cause the formation of proliferative foci, probably due to additional mutations that are a consequence of the accumulating DNA damage. We postulate that the same sort of DNA damage may result from the loss of BRCA1 *in vivo* and lead to tumor formation, and that this could be a more general model for related tumor suppressor systems.

Results

Targeting construct and abnormality of *Brcal* mutant mice

pBrcalneo (Figure 1a) was used to disrupt exon 11 which encodes about 60% of the amino acids of

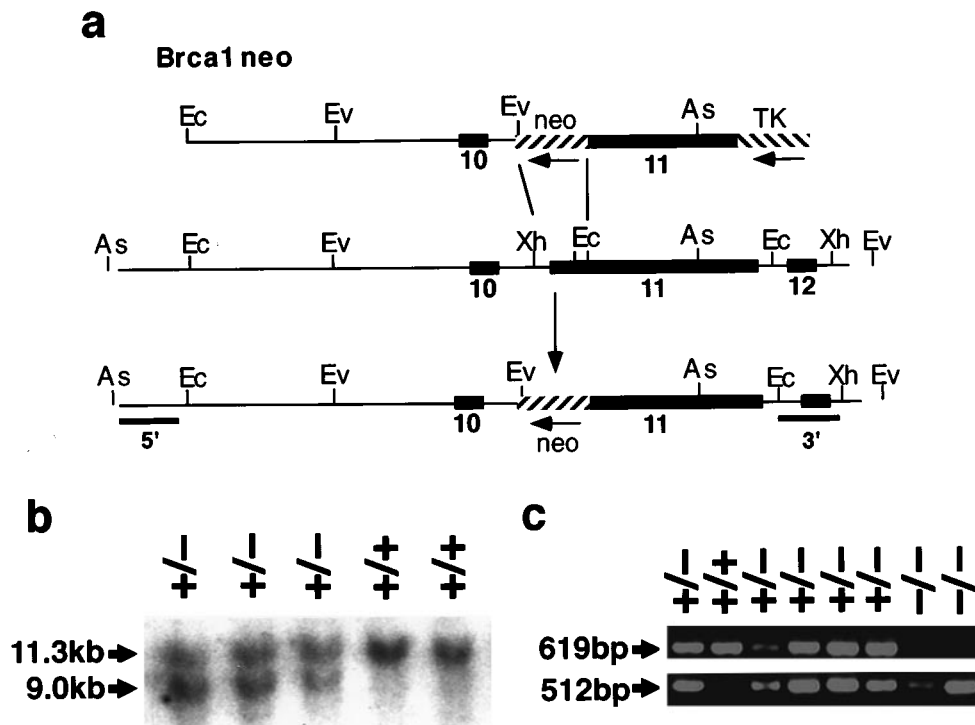


Figure 1 Targeted disruption of *Brca1* gene. (a) Targeting vector pBrca1neo contains a 9 kb *Brca1* genomic sequence with a pGKneo cassette (Tybulewicz *et al.*, 1991), that deletes a 0.74 kb *XhoI*–*EcoRI* segment. As, *Asp* 718; Ec, *EcoRI*; Ev, *EcoRV*; Xh, *XhoI*. (b) Southern blot analysis of DNAs isolated from a representative litter of pups generated by intercrosses between *Brca1*^{11+/-} mice. DNAs were digested by *EcoRV* and hybridized with the 3' flanking probe. The wild type (11.3 kb) and mutant (9 kb) fragments were as indicated. (c) PCR genotyping of a representative litter of E8.5. All abnormal embryos were homozygous for the targeted mutation

Table 1 Genotypes and morphology of embryos of offspring from crosses between *Brca1*^{11+/-} mice^a

Ages	Total decidua or pups	<i>Brca1</i> ^{11+/+}	<i>Brca1</i> ^{11+/-}	<i>Brca1</i> ^{11-/-}	Resorption ^d
E6.5	50	8	26	16	0
E7.5	63	11	39	11 ^b	2
E8.5	133	35	64	27 ^b	7
E9.5	101	27	53	14 ^c	7
E10.5	27	9	14	0	4
P20-8	69	26	43	0	

^aAll data shown in the table were obtained in the 50% 129 and 50% Black Swiss. E6.5-8.5 embryos were also analysed in the 50% 129 and 50% B6 C57 genetic background. Mutants in both backgrounds showed similar phenotypes. ^bEmbryos were both smaller and abnormal in morphology compared with their littermate controls. About one third of them were dead. ^cEmbryos showed variability in phenotype and over half of them were dead or dying. ^dEmbryos were nearly or completely resorbed and their genotype could not be reliably determined

murine BRCA1 (Bennett *et al.*, 1995; Lane *et al.*, 1995). Homologous recombination between the targeting construct and the endogenous counterpart would delete 330 bp of intron 10 and 407 bp of exon 11, including a splice acceptor for exon 11. A previous investigation showed that embryos carrying a similar deletion of this exon (330 bp of intron 10 plus 1.5 kb of exon 11) died at E9.5-13.5 (Gowen *et al.*, 1996). However, as summarized in Table 1, our *Brca1* mutant embryos (referred to as *Brca1*^{11-/-}) died at E7.5-9.5 and exhibited abnormalities sub-

stantially different from those described previously (Gowen *et al.*, 1996).

To assess the *Brca1*^{11-/-} phenotype, *Brca1*^{11+/-} mice were crossed to generate homozygotes. At E6.5, *Brca1*^{11-/-}, *Brca1*^{11+/-}, and *Brca1*^{+/+} embryos were present in a ratio of 1:2:1, and *Brca1*^{11-/-} embryos did not display apparent abnormalities (Table 1). However, at E7.5, *Brca1*^{11-/-} embryos ($n=11$) were found to be much smaller than their littermate controls (*Brca1*^{11+/-} and *Brca1*^{+/+} embryos) and looked like E6.5 embryos, suggesting that they were developmentally arrested at this stage (Figure 2a). At E8.5, about 1/3 of the *Brca1*^{11-/-} embryos were found dead. The others remained very small, resembling those found in E7.5 litters (Figure 2b). In histological sections, extraembryonic structures, such as the visceral yolk sac, and ectoplacental and exocoelomic cavities were significantly developed whereas embryonic portions lagged behind (Figure 2g). At E9.5, over half of *Brca1*^{11-/-} embryos were dying or dead. The remainder were abnormal and much smaller compared with the controls, indicating that the development of these embryos was severely affected (Figure 2c–e). A small portion (about 5%) of the *Brca1*^{11-/-} embryos were able to form non-axial mesodermal tissues, such as allantois, amnion, yolk sac and blood cells (Figure 2d and not shown). They could also form headfold-like structures, as revealed by expression of the *Otx-2* gene, a forebrain and midbrain marker (Figure 2k), although these embryos were abnormal. Whole mount *in situ*

hybridization of E9.5 *Brcal*^{11-/-} embryos with a probe for the *Brachyury* gene, which marks primitive streak and notochord of normal embryos, revealed a

delay in the formation of the primitive streak and an abnormal axial mesoderm in *Brcal*^{11-/-} embryos (Figure 2i).

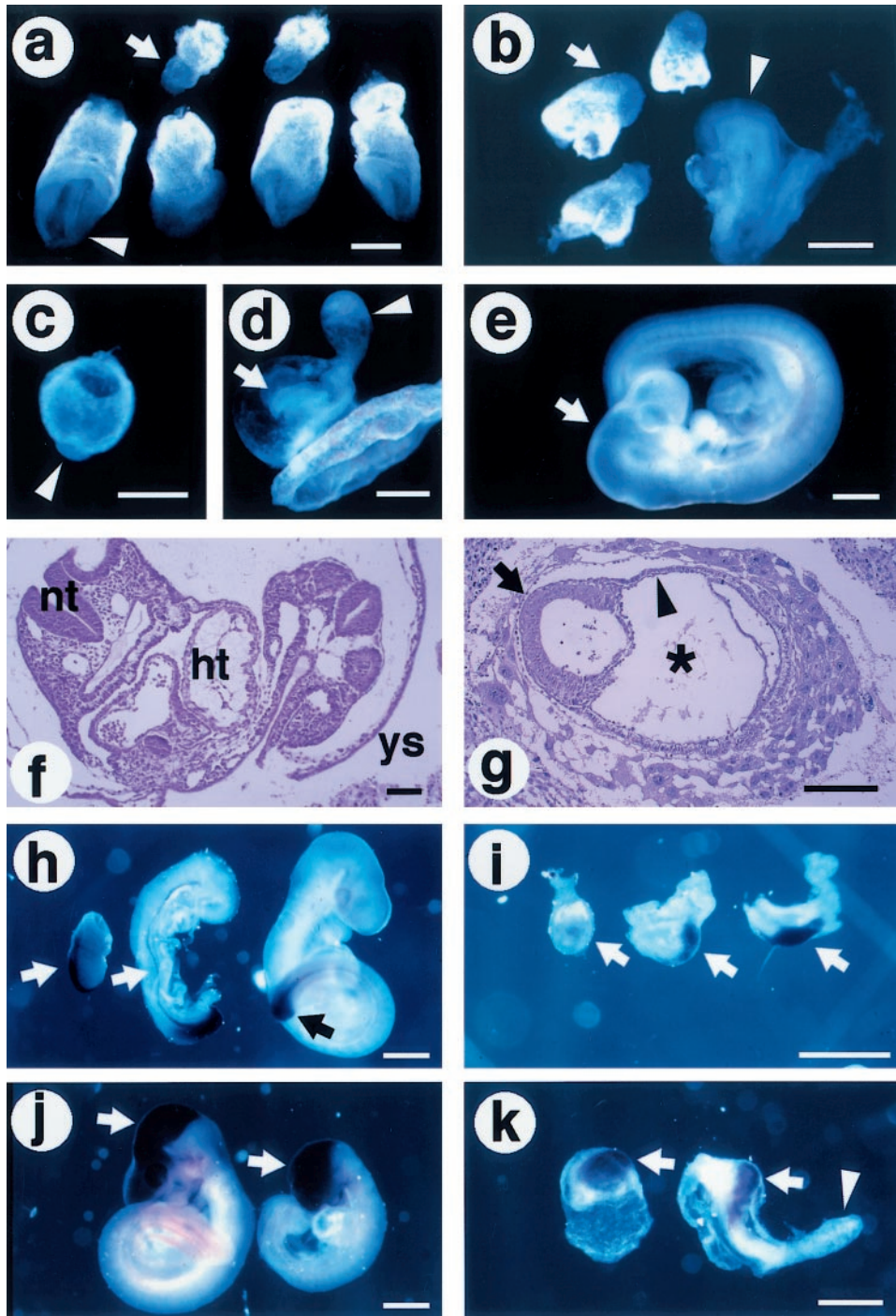


Figure 2 Molecular analysis of *Brcal*^{11-/-} embryos. (a) E7.5 embryos. The two *Brcal*^{11-/-} embryos (arrow) were developmentally retarded compared with their littermate controls (lower 4 embryos). (b) E8.5 embryos. The three *Brcal*^{11-/-} embryos (arrow) appeared similar to E7.5 *Brcal*^{11-/-} embryos except for the increased size of the extraembryonic portions. All five control embryos shown in (a and b) were either heterozygous or wild type for *Brcal*¹¹ mutation. Arrowheads point to their headfolds. (c-e) E9.5 embryos. Most mutant embryos were very small; (c) arrowhead points to embryonic portion compared with their littermates; (e) arrow points to the head. About 5% of the mutants (d) formed a headfold-like structure (arrow), allantois (arrowhead) and yolk sac. (f and g) Histological sections of E8.5 embryos. Neural tube (nt) and heart (ht) of control embryos (f) were clearly visible. The embryonic portion of mutant embryos (arrow in g) remained very small. The visceral yolk sac, and exocoelomic cavity are labeled by an arrowhead and an asterisk respectively. (h) and (i) *Brachyury* expression in control and mutant embryos. Primitive streak of the E7 (left arrow), notochord of E8.5 (middle arrow) and tail bud of E9.5 (black arrow) of control embryos are shown in (h). Three E9.5 mutant embryos are shown in (i). Domains that express the *Brachyury* are pointed to by arrows. (j and k) *Otx-2* expression in wild type (j) and mutant embryos (k) is indicated by arrows. Arrowhead in (k) points to allantois. White and black bars are 200 μm and 100 μm, respectively

Brcal^{11-/-} embryos are sensitive to γ -irradiation

It is known that BRCA1 and Rad51, a homolog of *E. coli* RecA that is involved in DNA damage repair (Muris *et al.*, 1993; Shinohara *et al.*, 1992, 1993), co-localize in the cell nucleus and interact with each other (Scully *et al.*, 1997b). Since *Rad51*^{-/-} embryos were hypersensitive to γ -irradiation (Lim and Hasty, 1996), we predicted that *Brcal*^{11-/-} embryos might have a similar phenotype if these two genes interact *in vivo*. To test this, blastocysts were isolated from *Brcal*^{11+/-} intercrosses and subjected to γ -irradiation with unirradiated embryos as controls. After treatment, both irradiated and unirradiated blastocysts were incubated in growth medium for up to 7 days. Without irradiation, cultured blastocysts of homozygous (*n*=13) and control (*n*=35) embryos showed no apparent differences in the outgrowth of trophoblast cells (TCs) (Figure 3a, b). However, a dramatic difference in the outgrowth of the inner cell mass (ICM) was observed between control and homozygotes (Figure 3a, b). As control ICMs increased in size significantly (Figure 3b), mutant ICMs remained very small (Figure 3a). It has been suggested that the TCs can survive because they are in a relatively

quiescent state and can undergo DNA endo-duplication, allowing them to tolerate spontaneous DNA damage (Lim and Hasty, 1996). However, after receiving irradiation at 300 rads, the growth of mutant TCs (*n*=10) was dramatically reduced, from 20–30 cells/embryo to 5–10 cells/embryo (Figure 3c), while control TCs (*n*=25) were only slightly reduced, from an 20–35 cells/embryo to 20–25 cells/embryo (Figure 3d).

Brcal^{11-/-} embryos show chromosomal instability

The hypersensitivity of *Brcal*^{11-/-} cells to γ -irradiation provided compelling evidence that BRCA1 is involved in DNA double-strand break repair (Ritter *et al.*, 1977). If this is the case, gross chromosomal changes should be observable in *Brcal*^{11-/-} embryos. The chromosome number and karyotype of *Brcal*^{-/-} embryos were therefore analysed. Examination of E7.5 control embryos indicated that over 97% of the cells contained 40 chromosomes (Table 2). In *Brcal*^{11-/-} embryos, about 70% of the cells maintained the normal chromosome number, and the remainder showed chromosomal abnormalities, containing less or more than 40 chromosomes per cell

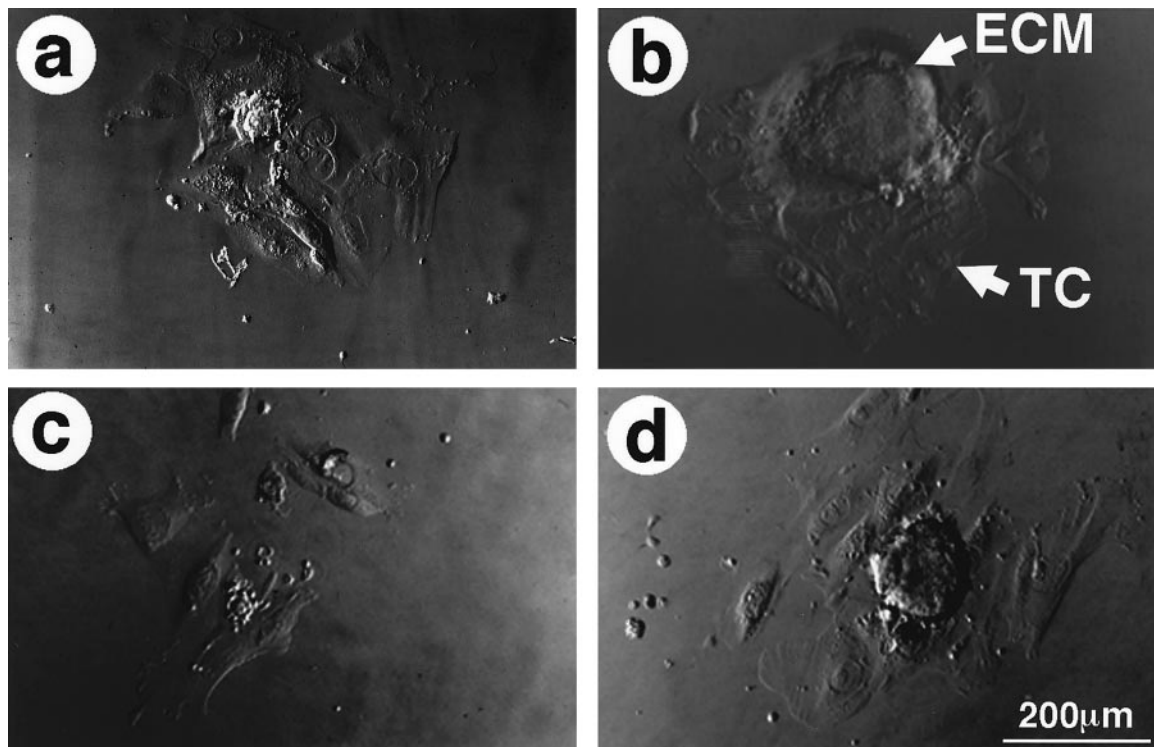


Figure 3 Hypersensitivity of *Brcal*^{11-/-} blastocysts to γ -irradiation. (a and b) unirradiated *Brcal*^{11-/-} (a) and control (b) blastocysts. (c and d) irradiated *Brcal*^{11-/-} (c) and control (d) blastocysts. Inner cell mass (ECM) and trophoblast cells (TC) were as indicated

Table 2 Chromosome abnormalities in *Brcal*^{11-/-} or *Brcal*^{11-/-} *p53*^{-/-} embryos

	Chromosome number/cell					Total # of metaphases	% Abnormal	# of Embryos
	> 50	41–50	40	35–39	< 35			
<i>Brcal</i> ^{+/+} or <i>Brcal</i> ^{+/-}	0	0	94	3	0	97	3.1	4
<i>Brcal</i> ^{-/-}	1	2	32	9	3	47	31.9	6
<i>Brcal</i> ^{+/-} <i>p53</i> ^{+/-}	0	0	40	0	1	41	2.4	1
<i>Brcal</i> ^{+/-} <i>p53</i> ^{-/-}	0	0	37	1	0	38	2.6	1
<i>Brcal</i> ^{-/-} <i>p53</i> ^{-/-}	13	9	21	20	13	76	72.4	2

(Table 2). The mitotic indices for control and *Brcal*^{11-/-} embryos are 31% (434 metaphases out of 1402 cells counted) and 5.3% (75 out of 1424 cells counted), respectively.

The chromosomal abnormalities are dramatically increased in a p53-null background

It was shown recently that the early lethality of BRCA1^{-/-} embryos could be partially rescued by a p53-null or p21-null mutation (Hakem et al., 1997; Ludwig et al., 1997). Since p53 is known to regulate the cell cycle through p21 (el-Deiry et al., 1993; Harper et al., 1993) we postulated that the rescue could be due to a failure in checkpoint control caused by the loss of these genes. If this is the case, a p53-null background should be more tolerant to the genetic instability in BRCA1^{-/-} cells and allow accumulation of mutations and DNA damage. To test this, we crossed p53-null mice (Donehower et al., 1992) with the *Brcal*^{11+/+} mice and analysed the resulting *Brcal*^{11-/-}:p53^{-/-} embryos. In the p53-null background, the *Brcal*^{11-/-} embryos survived on the average of 2 days longer, indicating that loss of p53 could partially rescue the BRCA1 deficiency. At E9.5, all *Brcal*^{11-/-}:p53^{-/-} were smaller and morphologically abnormal compared with their

littermates (Figure 4a, b). At E10.5, all double homozygous mutants were dying and partially deteriorated (not shown). We then prepared chromosome spreads from E9.5 *Brcal*^{11-/-}:p53^{-/-}, *Brcal*^{11+/+}:p53^{+/-} and *Brcal*^{11+/+}:p53^{-/-} embryos. We found that embryos with a functional *Brcal* gene contained 40 chromosomes, indicating that loss of p53 does not itself cause genetic instability at this stage of development (Table 2). In contrast, *Brcal*^{11-/-}:p53^{-/-} embryos displayed massive abnormalities. Of 76 metaphase spreads examined, 22 (29%) contained more than 40 chromosomes, and 33 (43%) contained less than 40 chromosomes (Table 2).

We wished to determine whether the embryonic cell metaphases contained structural abnormalities in addition to numerical changes. The chromosome spreads were subjected to spectral karyotyping (SKY), a recently developed molecular cytogenetic technique in which each chromosome is painted a different color by hybridization to fluorescent probes (Schrck et al., 1996). SKY allows an unambiguous identification of each chromosome, an extremely difficult task in early embryos by G- or DAPI-banding. No structural aberrations were observed in metaphases from *Brcal*^{+/+}:p53^{-/-} and *Brcal*^{11+/+}:p53^{-/-} embryos (not shown). In contrast, chromosomal rearrangements, including translocations and dicentric chromosomes, were found in *Brcal*^{11-/-}:p53^{-/-} (Figure 5a-d) and *Brcal*^{11-/-} (Figure 5e, f) embryos. Mutations varied from cell to cell even within a single embryo. Importantly, aberrations were observed even in the presence of a wild-type p53 allele.

Loss of p53 is not sufficient for Brcal^{-/-} cells to proliferate

The above data show that the loss of p53 partially rescued the BRCA1 deficiency at the expense of genomic integrity. It is conceivable that accumulating DNA damage could lead to the inactivation of genes that are essential for embryonic growth and patterning, leading to the death of *Brcal*^{11-/-}:p53^{-/-} embryos. However, it is not clear that the loss of p53 could rescue the BRCA1 deficiency at the cellular level. To address this, we derived mouse embryonic fibroblast cells (MEFs) from 5 E9.5 *Brcal*^{-/-}:p53^{-/-} and 14 control embryos (including those wild type for both genes). While all control MEFs grew vigorously and formed confluent monolayers quickly (Figure 4c), all five *Brcal*^{11-/-}:p53^{-/-} MEFs proliferated poorly at the primary passage. A majority of *Brcal*^{11-/-}:p53^{-/-} cells had enlarged cytoplasm and entered quiescent status (Figure 4d). With time, multiple foci were observed from all five cultured double mutant MEFs (Figure 4e, f). In the subsequent passages, three of *Brcal*^{11-/-}:p53^{-/-} MEFs reached passage 3 and one reached passage 5, but they all failed to proliferate further and died shortly thereafter, suggesting that they were not fully transformed. Because the *Brcal*^{11-/-}:p53^{+/-} and *Brcal*^{11-/-}:p53^{+/+} embryos died before E9.5, we derived MEFs from E8.5 *Brcal*^{11-/-}:p53^{+/-} and *Brcal*^{11-/-}:p53^{+/+} embryos (n=6) and found that the mutant cells could not grow even at the primary passage. Altogether, these data indicated that inactivation of p53 cell cycle control does not overcome the

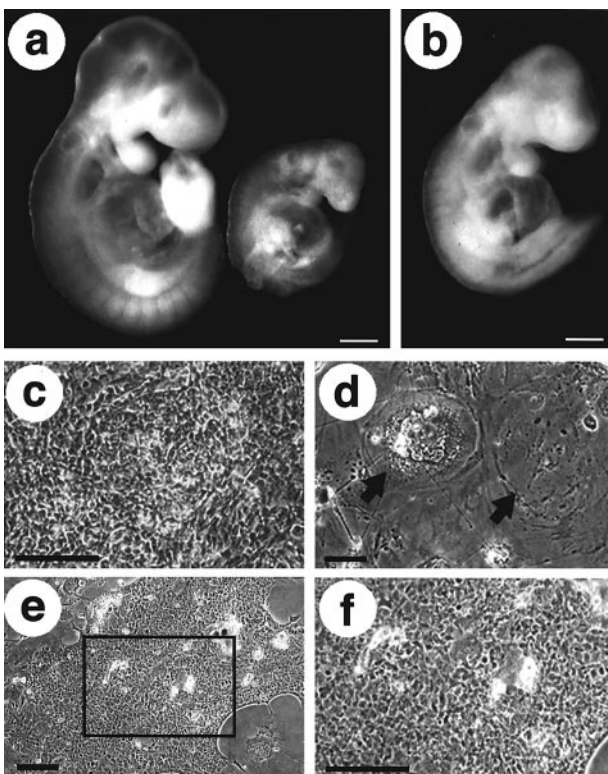


Figure 4 Loss of p53 partially rescues the *Brcal*^{11-/-} phenotypes. (a and b) E9.5 *Brcal*^{11-/-}:p53^{-/-} and control embryos. Both *Brcal*^{11-/-}:p53^{-/-} embryos (right embryo in a, b) were smaller than their control (left in a, b) and showed signs of deterioration. (c and f), Morphology of *Brcal*^{11-/-}:p53^{-/-} and control MEFs. All control MEFs (n=14) reached high density 3 days after plating (e), whereas *Brcal*^{11-/-}:p53^{-/-} MEFs (d) failed to grow and displayed enlarged cytoplasm with (left arrow) or without (right arrow) extensive vacuolization. Multiple foci were apparent from *Brcal*^{11-/-}:p53^{-/-} MEFs after 10 days in culture (e). An enlarged view of (e) was shown in (f). Bars are 100 μm

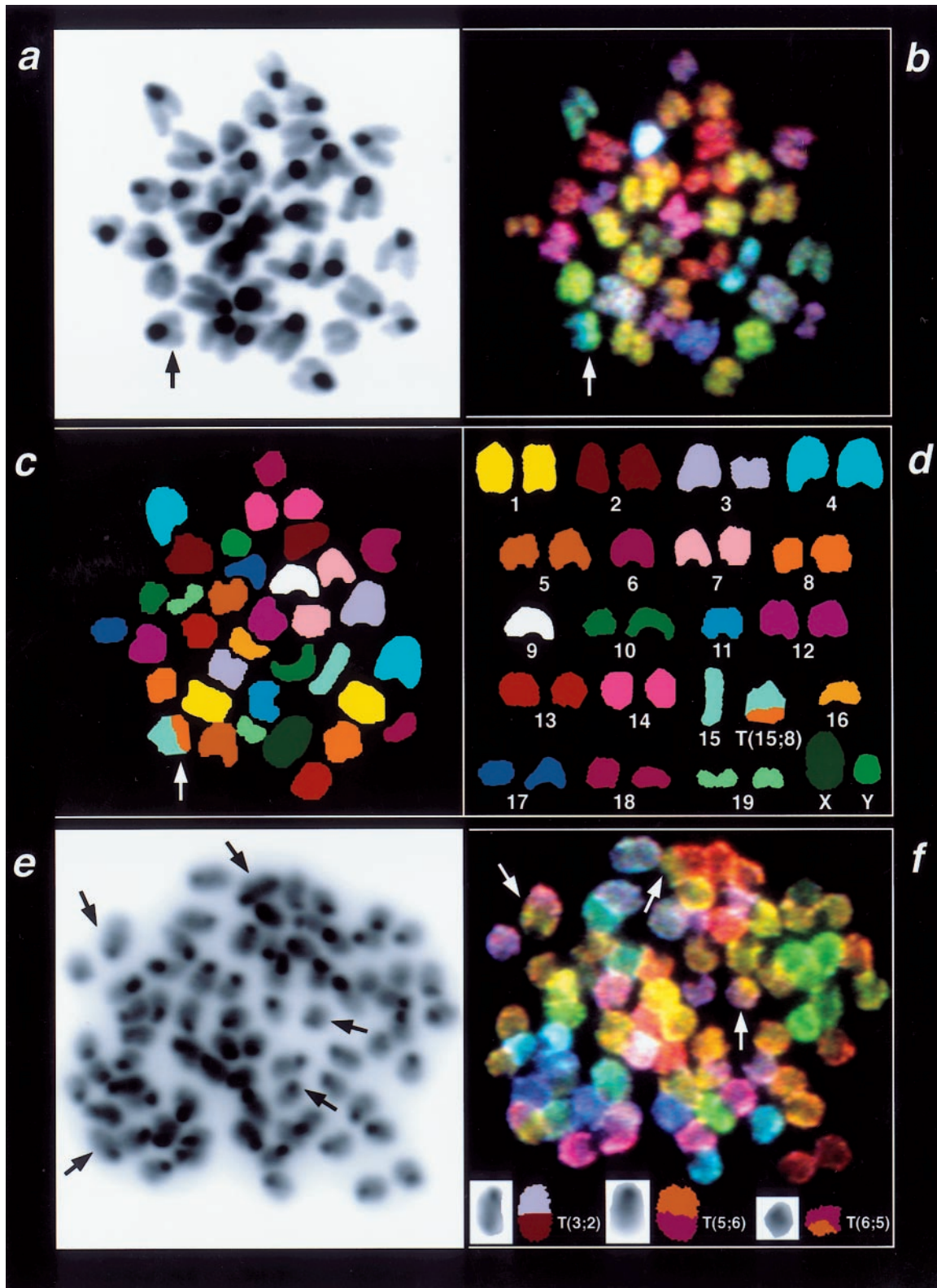


Figure 5 Chromosomal abnormalities revealed by SKY. (a) DAPI-stained metaphase from a *Brca1*^{-/-}; *p53*^{-/-} embryo. The aberrant chromosome is indicated by an arrow. (b) SKY of the same metaphase as in (a); the display colors shown were generated by applying red, green, or blue colors to different ranges of the spectrum (see Methods). (c) Spectral karyotype of the metaphase in (b) after spectra-based classification. Each chromosome was assigned a pseudocolor according to the measured spectrum, which allowed the determination of the karyotype (36,XY, T(15;8), -6,-9,-11) shown in (d). (e) DAPI-stained metaphase from a *Brca1*^{-/-}; *p53*^{+/-} embryo. The arrows denote all aberrant chromosomes detected by SKY. (f) SKY display image of the same metaphase shown in (e); arrows indicate the translocated chromosomes shown in their classification colors at the bottom of the image (the reciprocal translocations present in two copies are shown only once separately as classified images). This cell is hypotetraploid: 73,XX, T(3;2), T(5;6)x2, T(6;5)x2,-1,-2x2,-13,-16,-19x2

cellular defect caused by the loss of BRCA1. However, it does extend the survival of the *Brcal*^{11-/-} cells and allows further alteration to occur, which may eventually lead to malignant transformation.

Discussion

Previous investigations showed that targeted disruptions of the murine *Brcal* gene result in embryonic lethality from E6-13.5, depending on the site at which the mutation is introduced. Embryos homozygous for deletion of exon 2 (Ludwig *et al.*, 1997), exons 5-6 (Hakem *et al.*, 1996) or a deletion of a 184 bp *EcoRI* fragment within the 5' portion of exon 11 (Liu *et al.*, 1996) exhibited cellular proliferation defects and died before E8. In contrast, embryos carrying a deletion of a 1.8 kb *XhoI-KpnI* genomic fragment that contains 330 bp of intron 10 and 1.5 kb of exon 11 died at E9.5-13.5, displaying signs of both rapid proliferation and excessive cell death within the neural tube (Gowen *et al.*, 1996). Although the molecular basis for this discrepancy is unknown, it is conceivable that the removal of a splice acceptor site in the latter case may generate different splicing variants of *Brcal* that rescue the early post-implantation embryonic defects uncovered by the other studies (Ludwig *et al.*, 1997; Hakem *et al.*, 1996; Liu *et al.*, 1996). In the present study, our targeting construct deletes a 0.74 kb *XhoI-EcoRI-EcoRI* segment containing the same exon 11 splice acceptor that was deleted previously (Gowen *et al.*, 1996). However, the *Brcal*^{11-/-} embryos displayed abnormalities that are much more severe than those reported by Gowen *et al.* (1996). Because we also used the same strain background as Gowen *et al.* (1996), we believe that the genetic background is not the cause of the discrepancy. Notably, the phenotype of *Brcal*^{11-/-} embryos is similar to, but milder than those reported by the other studies (Ludwig *et al.*, 1997; Hakem *et al.*, 1996; Liu *et al.*, 1996). It was shown previously that deletion of exons 5 and 6 of the *Brcal* gene resulted in a dramatic increase in p21 transcription (Hakem *et al.*, 1997). However, we did not detect any obvious change in the p21 protein level in E6.5 *Brcal*^{11-/-} embryos by immunohistochemistry (not shown). While this discrepancy needs to be resolved by further study, it suggests that the targeted disruption of different domains of BRCA1 may cause a differential response of its downstream genes.

It has been speculated that BRCA1 is involved in DNA damage repair. The first hint of such a function of BRCA1 came from the observation that it co-localizes and co-immunoprecipitates with RAD51 (Scully *et al.*, 1997b). It was also shown that in response to treatment with DNA damaging reagents, BRCA1 became hyperphosphorylated and relocated along with RAD51 to intranuclear structures where DNA replication was taking place (Scully *et al.*, 1997a). RAD51 is involved in ATP-dependent DNA strand exchange reactions and is known to be a homolog of yeast RecA, which functions in homologous recombination and DNA damage repair (Ogawa *et al.*, 1993). We now provide additional evidence to support a role of BRCA1 in DNA damage repair by directly demonstrating that a loss-of-function mutation of BRCA1 results in chromosomal abnorm-

alities, including numerical and structural changes. It was shown that the most common damage caused by ionizing irradiation is double-strand breaks (DSB) of DNA (Ritter *et al.*, 1977). Thus, the hypersensitivity of *Brcal*^{11-/-} blastocysts to γ -irradiation may suggest a role of BRCA1 in the DSB repair.

Notably, another breast tumor suppressor gene, *Brcal2* exhibits many similarities to the *Brcal* gene. Like BRCA1, BRCA2 also co-localizes with RAD51 (Sharan *et al.*, 1997). BRCA2-null embryos are also hypersensitive to γ -irradiation and exhibit early embryonic lethality, which is partially rescued by a p53 mutation (Ludwig *et al.*, 1997). Moreover, embryos carrying hypomorphic alleles of BRCA2 exhibit chromosomal abnormalities similar to those seen in *Brcal*^{11-/-} and *RAD51*^{-/-} embryos (Patel *et al.*, 1998). The striking similarities between BRCA1 and BRCA2 suggest that these two proteins function in the same DNA repair process in which RAD51 is involved.

Despite the similarities, these two genes also exhibit differences. For example, BRCA2 has eight BRC motifs clustered in exon 11 (Wong *et al.*, 1997), which are lacking in BRCA1. The BRC motifs are conserved in BRCA2 proteins of different mammals from mice to human (Bignell *et al.*, 1997), suggesting that this domain is important for its function. Instead of BRC motifs, a conserved C-terminal domain of human and mouse BRCA1 proteins (BRCT) is also found in many nonorthologous proteins including 53BP1, RAD9, XRCC1 and others. Proteins with BRCT domain comprise a superfamily, and all of them appear involved in DNA damage responsive checkpoints (Bork *et al.*, 1997). In addition to a BRCT domain, a ring zinc finger found at the N-terminal of human and mouse BRCA1 suggests it has the ability to bind to DNA (Bienstock *et al.*, 1996) or another protein (Mackay and Crossley, 1998). Neither the BRCT domain nor the zinc finger have been found in BRCA2. These differences argue that BRCA1 and BRCA2 may have distinct functions in developmental processes.

Our data showed that *Brcal*^{11-/-} embryos exhibited both early post-implantation growth retardation and chromosomal abnormalities. Mouse embryos at early post-implantation stages undergo rapid cell proliferation with the epiblast cells increasing from 120 cells per E5.5 embryos to 660 cells per E6.5 embryos. The cell number increases further to 14290 per E7.5 embryo (Snow, 1977). Thus, we have considered a hypothesis that BRCA1 functions as a stimulus for embryonic cell proliferation. However, such a hypothesis could not explain the hypersensitivity to γ -irradiation and chromosomal abnormalities of the *Brcal*^{11-/-} embryos. Moreover, the early post-implantation growth retardation is rescued in a p53-null background, at the expense of a dramatic increase in chromosomal abnormalities. Altogether, these data indicate that the growth defect of *Brcal*^{11-/-} embryos is secondary to the observed genetic instability. p53 has been shown to be essential for the integrity of the genome (el-Deiry, 1998; Vogelstein and Kinzler, 1992). Upon treatment of reagents that damage DNA, p53 protein levels increase. Its C-terminal domain bind directly to the damaged DNA, allowing repair processes to initiate (Bakalkin *et al.*, 1994, 1995). p53 also activates its target genes such as p21, a CDK inhibitor, to prevent

cells that contain damaged DNA from proliferating (Deng *et al.*, 1995; el-Deiry *et al.*, 1993, 1994; Harper *et al.*, 1993; Waga *et al.*, 1994). However, if the damage is too extensive to be repaired, p53 triggers expression of proteins that promote apoptosis, such as Bax, to eliminate the cells that contain the damage (Miyashita and Reed, 1995). Based on our analysis of the *Brcal*^{11-/-} embryos, we propose that BRCA1 plays an indispensable role in the DNA repair machinery in concert with RAD51. In the normal situation, the embryonic cells can efficiently repair spontaneous DNA damage associated with the rapid proliferation of the early post-implantation embryos. The loss of BRCA1 in these cells results in genetic instability, triggering a p53 mediated cell cycle checkpoint, which restrains the cells from proliferating and prevents accumulation of un-repaired DNA. This checkpoint is abolished in *Brcal*^{11-/-};p53^{-/-} embryos, allowing accumulation of massive chromosomal abnormalities.

In summary, we showed that *Brcal*^{11-/-} embryos were hypersensitive to γ -irradiation and displayed massive abnormalities in chromosome number and structure when they were placed on a p53-null background. These findings directly illustrate the role of BRCA1 in maintaining the stability of the genome and provide some insights regarding the mechanism by which BRCA1 suppresses tumor formation. Notably, tumorigenesis in people with BRCA1 mutations occurs with relatively long latency and somatic mutations are rarely detected in sporadic cases (Easton, 1997; Futreal *et al.*, 1994; Struewing *et al.*, 1997; Xu and Solomon, 1996). In light of our findings, we believe that this is primarily because the loss of BRCA1 does not directly promote tumorigenesis. Our observation that the inactivation of p53 itself is not sufficient to allow BRCA1 cells to proliferate but does cause formation of multiple proliferative foci suggests a involvement of multiple factors in the BRCA1 associated tumorigenesis. This may account for the relatively long latency of cancer incidence in people carrying *Brcal* mutations and the rare incidence of somatic *Brcal* mutations in sporadic cancers (Easton, 1997; Futreal *et al.*, 1994; Struewing *et al.*, 1997; Xu and Solomon, 1996).

Materials and methods

Targeting vector

Recombinant phages containing genomic DNA of the *Brcal* locus were isolated from a 129 mouse library (Stratagene). To construct the targeting vector for *Brcal*, a 6 kb *EcoRI*-*XhoI* fragment that is 5' to exon 11 of the *Brcal* gene was subcloned into the *XbaI* and *EcoRI* sites of pPNT (Tybulewicz *et al.*, 1991). The resulting construct was cleaved with *XhoI* and *NotI*, followed by insertion of a 3 kb *EcoRI*-*NotI* fragment (the *NotI* site is from the polylinker of the phage vector). The finished construct, *pBrcalNeo*, is shown in Figure 1a.

Homologous recombination in ES cells and generation of germline chimeras

TC1 ES cells (Deng *et al.*, 1996) were transfected with *NotI* digested *pBrcalNeo* and selected with G418 and FIAU. The culture, electroporation, and selection of TC1 cells was carried out as described (Deng *et al.*, 1995). Genomic DNAs from G418^r/FIAU^r clones and the

parental TC1 cell line were digested with *Asp718* and then probed with a 5' fragment, or digested with *EcoRV* and probed with a 3' probe. The 5' probe is a 1.2 kb *EcoRI* fragment and the 3' fragment is a 1 kb *EcoRI*-*XhoI* fragment. Of 156 of G418 and FIAU double-resistant ES clones analysed for homologous recombination, 18 contained correct targeting events. Germline transmission was obtained from injection of three ES clones into C57BL/6J blastocysts.

Mating and genotyping mice

Chimeric mice were mated with NIH Black Swiss females (Taconic), C57B6 or 129SvEv. Agouti offspring were tested for the presence of the *Brcal* allele by Southern analysis or PCR. For PCR analysis, the wild type *Brcal* allele was detected by using a 5' oligonucleotide (5'-CAAA-CAGCCTGGCATAGCAG-3') and a 3' oligonucleotide (5'-GATGAAGTCCTCAGGTTGAAG-3'). This primer pair flanks the *PGKneo* insertion site, and amplifies a 618 bp fragment from the wild type *Brcal* gene. DNA was also amplified using the 3' primer and a primer specific to *PGKneo* (5'-CCAGACTGCCTTGGGAAAAGC-3'). In this case, a fragment of about 730 bp is detected in mice heterozygous or homozygous for the *Brcal*¹¹ allele, while no signal can be detected in wild type mice. p53-deficient mice (Donehower *et al.*, 1992) were mated with *Brcal*^{11+/-} to generate *Brcal*^{11+/-};p53^{-/-} mice which were then interbred to generate *Brcal*^{11-/-};p53^{-/-} embryos.

In vitro culture and irradiation of blastocysts

Conditions for blastocyst culture were as described (Deng *et al.*, 1994). On day 0, blastocysts were either irradiated by a γ -generator at a dose of 300 rads or 0 rad (untreated) before the initiation of the culture. The blastocysts of both groups were subsequently transferred individually into each well of 24-well culture plates containing growth medium. Photographs of cultured embryos were taken from day 3 through day 7 at the same magnification. Cells were harvested and DNAs were extracted for genotype analysis by PCR on day 7. The number of trophoblast-like cells (TCs) were counted and the area of inner cell mass (ICM) was measured by NIH image. The data were examined by Student's *t*-test.

Mouse embryonic fibroblast cell (MEF) culture

Primary MEFs were obtained from E9.5 embryos that were *Brcal*^{11-/-};p53^{-/-} and controls (*Brcal*^{11+/-};p53^{-/-}, *Brcal*^{11+/+};p53^{-/-}, *Brcal*^{11+/+};p53^{+/-} or *Brcal*^{11+/-};p53^{+/-}). Because the *Brcal*^{11-/-} embryos in p53^{+/-} or p53^{+/-} backgrounds died before E9.5, we derived *Brcal*^{11-/-};p53^{+/-} and control cells at E8.5. Individual embryo was trypsinized at room temperature for 10 min and plated into one well of 12-well (for E9.5 embryos) or 24-well (for E8.5 embryos) plates. MEFs from all control embryos filled the well quickly and were passed into a larger well at each subsequent passage. Foci from *Brcal*^{11-/-};p53^{-/-} cells were generally passed into wells of same size (24-well plate) in the subsequent passages. Only in two cases, the *Brcal*^{11-/-};p53^{-/-} cells reached about 70% confluence and they were passed into 12-well plates.

Chromosome preparations from and spectral karyotyping of mouse embryos

Chromosomes of mouse embryos were prepared following the approach described by EP Evans (1987) with minor modifications. The E.7.5-E.9.5 embryos were dissected

and cultured in complete medium with 0.1 $\mu\text{g/ml}$ Colcemid (Sigma) for 8 h at 37°C. The embryos were treated with 1% tri-sodium citrate for 20 min and then fixed with 3:1 mixture of methanol:acetic acid. The embryos were then processed as described.

Spectral karyotyping of the embryonic cell metaphases was performed as described previously for human and mouse (Schröck *et al.*, 1996; Liyanage *et al.*, 1996). Briefly, flow-sorted mouse chromosomes were amplified by degenerate oligonucleotide-primed PCR incorporating haptenized or fluorochrome-conjugated nucleotides (Telenius *et al.*, 1992). The degenerate primer sequence used was: 5'-CGGACTC-GAGNNNNNTACACC-3'. The resulting chromosome-specific painting probes were hybridized to the metaphase chromosomes (described above) on glass slides for 2–3 days, in the presence of a large excess of unlabeled Cot-1 fraction of mouse genomic DNA (kindly provided by M Liyanage). Slides were washed in 50% formamide/1 \times SSC to detect nucleotides directly labeled with Rhodamine 110 (Applied Biosystems), Spectrum Orange (Vysis) and Texas Red (Molecular Probes); additionally, biotin and digoxigenin indirectly-labeled nucleotides were detected with Cy5 and Cy5.5 conjugates (Amersham), respectively. Chromosomes were counterstained with DAPI. Spectral analysis of chromosomes was carried out on a microscope (Leica DMRBE) that was equipped with a SD200 spectral cube

(Applied Spectral Imaging) and a custom-designed filter cube (Chroma Technology) that allows for the simultaneous excitation of all dyes and the measurement of their emission spectra. Analysis of the images was performed using SkyView software (Applied Spectral Imaging). To visualize the raw spectral image, different colors (blue, green, or red) were assigned to specific spectral ranges. Chromosomes then were unambiguously identified using a spectral classification algorithm that results in the assignment of a separate classification color to all pixels with identical spectra.

Acknowledgements

We are indebted to Philip Leder, in whose laboratory this work was initiated. We thank J Rossant for *Otx-2* probe, L Donehower for the p53^{-/-} mice, Z Liu for technical assistance, and members of Deng laboratory for comments on the manuscript.

References

- Alberg AJ and Helzlsouer KJ. (1997). *Curr. Opin. Oncol.*, **9**, 505–511.
- Bakalkin G, Selivanova G, Yakovleva T, Kiseleva E, Kashuba E, Magnusson KP, Szekely L, Klein G, Terenius L and Wiman KG. (1995). *Nucleic Acids Res.*, **23**, 362–369.
- Bakalkin G, Yakovleva T, Selivanova G, Magnusson KP, Szekely L, Kiseleva E, Klein G, Terenius L and Wiman KG. (1994). *Proc. Natl. Acad. Sci. USA*, **91**, 413–417.
- Bennett LM, Haugen-Strano A, Cochran C, Brownlee HA, Fiedorek Jr FT and Wiseman RW. (1995). *Genomics*, **29**, 576–581.
- Bienstock RJ, Darden T, Wiseman R, Pedersen L and Barrett, JC. (1996). *Cancer Res.*, **56**, 2539–2545.
- Bignell G, Micklem G, Stratton MR, Ashworth A and Wooster R. (1997). *Hum. Mol. Genet.*, **6**, 53–58.
- Bork P, Hofmann K, Bucher P, Neuwald AF, Altschul SF and Koonin EV. (1997). *Faseb. J.*, **11**, 68–76.
- Casey G. (1997). *Curr. Opin. Oncol.*, **9**, 88–93.
- Deng C, Wynshaw-Boris A, Zhou F, Kuo A and Leder P. (1996). *Cell*, **84**, 911–921.
- Deng C, Zhang P, Harper JW, Elledge SJ and Leder P. (1995). *Cell*, **82**, 675–684.
- Deng CX, Wynshaw-Boris A, Shen MM, Daugherty C, Ornitz DM and Leder P. (1994). *Genes Dev.*, **8**, 3045–3057.
- Donehower LA, Harvey M, Slagle BL, McArthur MJ, Montgomery Jr CA, Butel JS and Bradley A. (1992). *Nature*, **356**, 215–221.
- Easton D. (1997). *Nat. Genet.*, **16**, 210–211.
- El-Deiry WS. (1998). *Curr. Top. Microbiol. Immunol.*, **227**, 121–137.
- El-Deiry WS, Harper JW, O'Connor PM, Velculescu VE, Canman CE, Jackman J, Pietenpol JA, Burrell M, Hill DE, Wang Y, Wiman KG, Mercer WE, Kastan MB, Kohn KW, Elledge SJ, Kinzler KW and Vogelstein B. (1994). *Cancer Res.*, **54**, 1169–1174.
- El-Deiry WS, Tokino T, Velculescu VE, Levy DB, Parsons R, Trent JM, Lin D, Mercer WE, Kinzler KW and Vogelstein B. (1993). *Cell*, **75**, 817–825.
- Evans EP. (1987). *Mammalian Development*. Monk, M. (ed). IRL Press: Oxford, pp 93–114.
- Futreal PA, Liu Q, Shattuck-Eidens D, Cochran C, Harshman K, Tavtigian S, Bennett LM, Haugen-Strano A, Swensen J, Miki Y, Eddington K, McClure M, Frye C, Weaver-Feldhaus J, Ding W, Gholami Z, Söderkvist P, Terry L, Jhanwar S, Berchuck A, Iglehart JD, Marks J, Ballinger DG, Barrett JC, Skolnick MH, Kamb A and Wiseman R. (1994). *Science*, **266**, 120–122.
- Gowen LC, Johnson BL, Latour AM, Sulik KK and Koller BH. (1996). *Nat. Genet.*, **12**, 191–194.
- Hakem R, de la Pompa JL, Elia A, Potter J and Mak TW. (1997). *Nat. Genet.*, **16**, 298–302.
- Hakem R, de la Pompa JL, Sirard C, Mo R, Woo M, Hakem A, Wakeham A, Potter J, Reitmair A, Billia F, Firpo E, Hui CC, Roberts J, Rossant J and Mak TW. (1996). *Cell*, **85**, 1009–1023.
- Harper JW, Adami GR, Wei N, Keyomarsi K and Elledge SJ. (1993). *Cell*, **75**, 805–816.
- Hill AD, Doyle JM, McDermott EW and O'Higgins NJ. (1997). *Br. J. Surg.*, **84**, 1334–1339.
- Lane TF, Deng C, Elson A, Lyu MS, Kozak CA and Leder P. (1995). *Genes Dev.*, **9**, 2712–2722.
- Lim DS and Hasty P. (1996). *Mol. Cell. Biol.*, **16**, 7133–7143.
- Liu CY, Flesken-Nikitin A, Li S, Zeng Y and Lee WH. (1996). *Genes Dev.*, **10**, 1835–1843.
- Liyanage M, Coleman A, du Manoir S, Veldman T, McCormack S, Dickson RB, Barlow C, Wynshaw-Boris A, Janz S, Wienberg J, Ferguson-Smith MA, Schröck E and Ried T. (1996). *Nat. Genet.*, **14**, 312–315.
- Ludwig T, Chapman DL, Papaioannou VE and Efstratiadis A. (1997). *Genes Dev.*, **11**, 1226–1241.
- Mackay JP and Crossley M. (1998). *Trends Biochem. Sci.*, **23**, 1–4.

- Miki Y, Swensen J, Shattuck-Eidens D, Futreal PA, Harshman K, Tavtigian S, Liu Q, Cochran C, Bennett LM, Ding W, Bell R, Rosenthal J, Hussey C, Tran T, McClure M, Frye C, Hattier T, Phelps R, Haugen-Strano A, Katcher H, Yakumo K, Gholami Z, Shaffer D, Stone S, S Bayer, Wray C, Bogden R, Dayananth P, Ward J, Tonin P, Narod S, Bristow PK, Norris FN, Helvering L, Morrison P, Rosteck P, Lai M, Barrett JC, Lewis C, Neuhausen S, Cannon-Albright L, Goldgar D, Wiseman R, Kamb A and Scolnick MH. (1994). *Science*, **266**, 66–71.
- Miyashita T and Reed JC. (1995). *Cell*, **80**, 293–299.
- Muris DF, Vreeken K, Carr AM, Broughton BC, Lehmann AR, Lohman PH and Pastink A. (1993). *Nucleic Acids Res.*, **21**, 4586–4591.
- Ogawa T, Shinohara A, Nabetani A, Ikeya T, Yu X, Egelman EH and Ogawa H. (1993). *Cold Spring Harb. Symp. Quant. Biol.*, **58**, 567–576.
- Patel KJ, Yu VPCC, Lee H, Corcoran A, Thistlethwaite FC, Evans MJ, Colledge WH, Friedman LS, Ponder BR and Venkitaraman AR. (1998). *Mol. Cell.*, **1**, 347–357.
- Ritter MA, Cleaver JE and Tobias CA. (1977). *Nature*, **266**, 653–655.
- Schreck E, du Manoir S, Veldman T, Schoell B, Wienberg J, Ferguson-Smith MA, Ning Y, Ledbetter DH, Bar-Am I, Soenksen D, Garini Y and Ried T. (1996). *Science*, **273**, 494–497.
- Scully R, Chen J, Ochs RL, Keegan K, Hoekstra M, Feunteun J and Livingston DM. (1997a). *Cell*, **90**, 425–435.
- Scully R, Chen J, Plug A, Xiao Y, Weaver D, Feunteun J, Ashley T and Livingston DM. (1997b). *Cell*, **88**, 265–275.
- Sharan SK, Morimatsu M, Albrecht U, Lim DS, Regel E, Dinh C, Sands A, Eichele G, Hasty P and Bradley A. (1997). *Nature*, **386**, 804–810.
- Shinohara A, Ogawa H, Matsuda Y, Ushio N, Ikeyo K and Ogawa T. (1993). *Nat. Genet.*, **4**, 239–243.
- Shinohara A, Ogawa H and Ogawa T. (1992). *Cell*, **69**, 457–470.
- Snow MHL. (1977). *J. Embryol. Exp. Morphol.*, **42**, 293–303.
- Struwing JP, Hartge P, Wacholder S, Baker SM, Berlin M, McAdams M, Timmerman MM, Brody LC and Tucker MA. (1997). *N. Engl. J. Med.*, **336**, 1401–1408.
- Telenius H, Pelmeur AH, Tunnacliffe N, Carter NP, Behmel A, Ferguson-Smith MA, Nordenskjold M, Pfragner R and Ponder BAJ. (1992). *Genes Chrom. Cancer*, **4**, 257–263.
- Tybulewicz VL, Crawford CE, Jackson PK, Bronson RT and Mulligan RC. (1991). *Cell*, **65**, 1153–1163.
- Vogelstein B and Kinzler KW. (1992). *Cell*, **70**, 523–526.
- Waga S, Hannon GJ, Beach D and Stillman B. (1994). *Nature*, **369**, 574–578.
- Wong AKC, Pero R, Ormonde PA, Tavtigian SV and Bartel PL. (1997). *J. Biol. Chem.*, **272**, 31941–31944.
- Wooster R, Bignell G, Lancaster J, Swift S, Seal S, Mangion J, Collins N, Gregory S, Gumbs C and Micklem G. (1995). *Nature*, **378**, 789–792.
- Xu CF and Solomon E. (1996). *Semin. Cancer Biol.*, **7**, 33–40.